ELSEVIER

Journal of Nuclear Materials 258–263 (1998) 1259–1263

journal of nuclear materials

The effect of low dose irradiation on the impact fracture energy and tensile properties of pure iron and two ferritic martensitic steels

I. Belianov [a], P. Marmy [b,*]

[a] *Central Research Institute for Structural Materials, Prometey, Sankt-Petersburg, 193167, Russian Federation*

[b] *Technologie de la Fusion Association Euratom-Confédération Suisse Centre de Recherche en Physique des Plasmas, Ecole Polytechnique Fédérale de Lausanne, CH-5232 Villigen-PSI, Switzerland*

Abstract

Two batches of subsize V-notched impact bend specimens and subsize tensile specimens have been irradiated in the Saphir test reactor of the Paul Scherrer Institute (PSI). The first batch of specimen has been irradiated at 250°C to a dose of 2.65×10^{19} n/cm^2 (0.042 dpa) and the second batch has been irradiated at 400°C to a dose of 8.12×10^{19} n/cm^2 (0.13 dpa). Three different materials in three different microstructures were irradiated: pure iron and two ferritic steels, the alloy MANET 2 and a low activation composition CETA. The results of the impact tests and of the corresponding tensile tests are presented. Despite the very low neutron dose, a significant shift of the ductile to brittle transition temperature (DBTT) is observed. The influence of the test temperature on the impact energy is discussed for the irradiated and unirradiated conditions, with special emphasis on the microstructure.

1. Introduction

Although ferritic martensitic steel is today a promising material for fusion reactors, many problems still exist [1], among them the rise of the ductile to brittle transition temperature (DBTT) after irradiation. The existence of DBTT is an intrinsic property of body-centered cubic ferrous alloys. The variables that affect the transition temperature are numerous. The chemical composition is important and elements like carbon and phosphorous are detrimental and will increase it, manganese on the contrary can lower it. The microstructure is another parameter that is strongly affecting the transition temperature.

This work describes qualitatively the effect of neutron irradiation on the DBTT in three distinct and characteristic microstructures, using Charpy V-notch specimen. The microstructures tested are ferrite, virgin martensite and tempered martensite. The change in the tensile properties due to the irradiation is compared with the change observed in the DBTT. The irradiations were carried out in the Saphir test reactor at the Paul Scherrer Institute (PSI) using an irradiation rig with gas loop.

2. Experimental

2.1. Specimen, materials and microstructures

The impact specimen used is a subsize $3 \times 4 \times 27$ mm^3 specimen of type DIN 50115, KLST with a V-notch of 1 mm parallel to the 3 mm edge. The tensile specimen is a DIN 50125, B3 × 15 specimen with a gage length of 18 mm and a diameter of 3 mm. The specimen was machined in the rolling direction. The chemical analysis of the materials is given in Table 1. The iron used is ARMCO iron as it was the only pure iron (99.9%) available in the dimensions necessary to manufacture the specimen. The iron was tested in the as received condition: hot rolled, air cooled and surface

* Corresponding author. Fax: +41 310 45 29; e-mail: pierre.marmy@psi.ch.

0022-3115/98/$19.00
PII: S0022-3115(98)00193-7

Table 1
The chemical analysis (wt%) of the tested materials

	IRON	CETA	MANET 2
C	0.005	0.17	0.11
Mn	0.04	1.35	1.22
P	0.003	0.008	0.005
S	0.002	0.004	0.004
Cu	0.008	0.012	0.008
N	0.004	0.015	0.039
Cr	–	9.6	10.3
Ni	–	–	0.62
W	–	0.81	–
Mo	–	–	0.57
Ta	–	0.48	–
Ce	–	0.13	–
Nb	–	–	0.14

finished. The structure is an α ferrite in fine grains. The MANET steel was austenitized at 1075°C for 30 min, air cooled and then tempered for 2 h at 750°C to give a final structure of martensite laths decorated by carbides. The alloying elements (V, Nb, Cr, Mo, Ni) are used partially to form the precipitate [2]. The CETA steel, a low activation evolution of MANET 2 [3], was austenitized at 1075°C for 30 min, air cooled to produce a high strength martensite with a very high internal dislocation density. Most of the alloying elements remain in solution. This type of structure has interstitial carbon occupying the octahedral sites of the bcc lattice but even in a rapid quench the carbon can escape and segregate to the dislocations, thus pinning the dislocations [4]. The mean grain size of the studied materials was 58 μm for iron, 28 μm for CETA and 30 μm for MANET 2.

2.2. Tensile and impact tests

The tensile tests were performed with a servo-mechanical machine of type RMC100, equipped with a vacuum furnace. The deformation rate in all tests was 2.5×10^{-4} s^{-1}. The impact tests were realized with a fully instrumented Messtek–Amsler PHR1010 charpy machine equipped with an automatic loading, heating and cooling system SFL-R1050. The kinetic energy available at impact was 30 J and the tup speed was 3.59 m/s. The DBTT was taken as the temperature at which one-half of the upper shelf energy was absorbed.

2.3. Irradiations

Two irradiation rigs intended to run at two different temperatures, 250°C and 400°C and denominated respectively as LAM 1 and LAM 2, were placed at the edge of the Saphir core. The counting of the dosimetry detectors placed in the rigs delivered a dose of 2.65×10^{23} nm^{-2} (0.042 dpa) for the LAM 1 irradiation and 8.12×10^{23} nm^{-2} (0.13 dpa) for the LAM 2 irradiation. The flux was of the order of 10^{13} ncm^{-2} s^{-1} which is in good agreement with calculations made with the BOXER code [5]. The mean temperatures of LAM1 and LAM 2 were 265°C(±15°C) and 405°C(±15°C).

3. Results and discussion

3.1. Tensile tests

3.1.1. Iron

The engineering tensile curves for pure iron unirradiated and irradiated in LAM 1 and 2 are shown in Fig. 1(a) and (b). The $\sigma_{0.2}$ offset yield stress of the unirradiated material decreases as the test temperature increases, showing a plateau around 250°C. This can be deduced from the figures obtained for $\sigma_{0.2}$ which are 223, 206 and 168 MPa respectively at RT, 250°C and 400°C (see Table 2). The maximum flow stress increases with

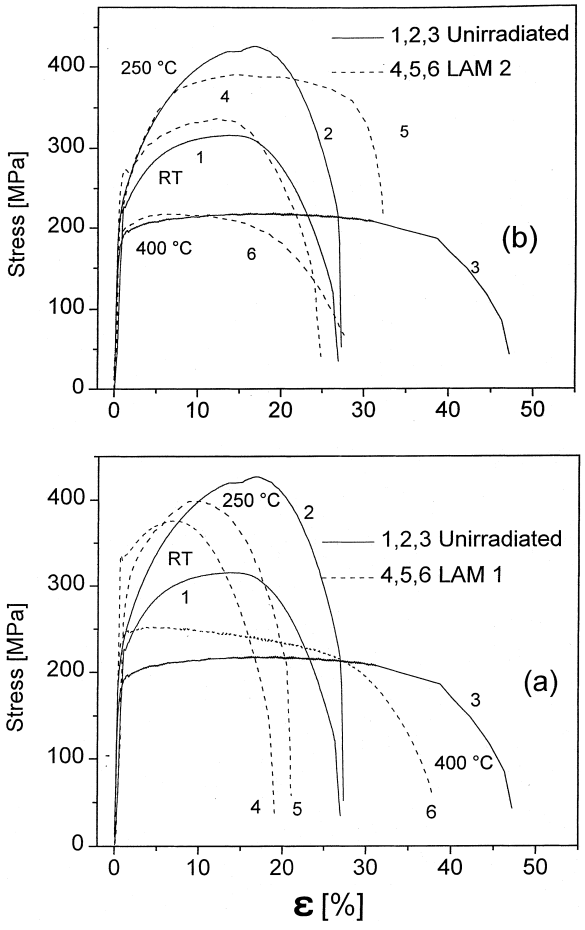

Fig. 1. The tensile curves of iron for the LAM 1 irradiation (a) and the LAM 2 irradiation (b) Test temperatures: 1&4, RT, 2&5, 250°C, 3&6, 400°C.

Table 2
Tensile stresses in Mpa of iron, Manet 2, and CETA in the case of LAM 1, as a function of the test temperature

	Armco iron			Manet 2 as received			CETA as quenched		
	RT	250°C	400°C	RT	250°C	400°C	RT	250°C	400°C
σ_m	316	420	219	775	672	631	1410	1440	1400
$\sigma_{0.2}$	223	206	168.5	671	579	565	1047	1074	1085
$\Delta\sigma_{irr,\,m}$	60	−28	34	64	50	34	40	8	60
$\Delta\sigma_{irr,0.2}$	111	55	59	93	85	37	243	95	63

temperature up to approximately 250°C and then decreases again. This behaviour of the yield and flow stress has been reported earlier, for instance by Dingley et al. [6] and can be explained by the increased diffusity of interstitial carbon above 100°C and the ability of these atoms to be attracted by the stress field of the moving dislocations, thus impeding their motion and producing an higher hardening rate. The observation of dynamic strain ageing in this temperature domain is consistent with this mechanism.

The effect of the LAM 1 irradiation on the ultimate stress σ_m and yield stress $\sigma_{0.2}$ of Armco iron is given in Table 2. The irradiation hardening derived from the change of the yield stress decreases up to a temperature of 250°C and then remains constant. The ultimate stress σ_m indeed is clearly reduced at a test temperature of 250°C. The same behaviour is produced by the LAM 2 ($T_{irr} = 400$°C) irradiation, although the irradiation hardening for the three times higher dose is smaller and the reduction of the flow stress $\sigma(\varepsilon)$ at 250°C is larger (Fig. 1). A strong reduction of the flow instabilities was observed, particularly in the LAM 2 specimen.

3.1.2. MANET 2 and CETA

The tensile curves for the MANET 2 steel are shown in Fig. 2(a) and (b) for the LAM 1 and LAM 2 irradiations respectively. The effect of the irradiation is to increase the yield and the flow stress for all test temperatures. The irradiation has little effect on the uniform elongation for both LAM 1 and LAM 2 irradiation. The total elongation is barely affected. The effect on the yield and ultimate stresses is given in Table 2 for the case of LAM 1 ($T_{irr} = 250$°C).

The CETA steel irradiated in the quenched condition is showing irradiation hardening at all test temperatures, in the case of the LAM 1 low temperature irradiation. On the contrary the LAM 2 irradiation performed at an elevated temperature (405°C for approximately 1700 h) produces some softening due to a recovery of the very high dislocation density during the exposure in the rig. Surprisingly despite the very high strength level (1500 Mpa), for all conditions, the total ductility remains above 10% and the uniform elongation above 4.5%. The effects of the LAM 1 irradiation on the tensile stresses of CETA are given in Table 2.

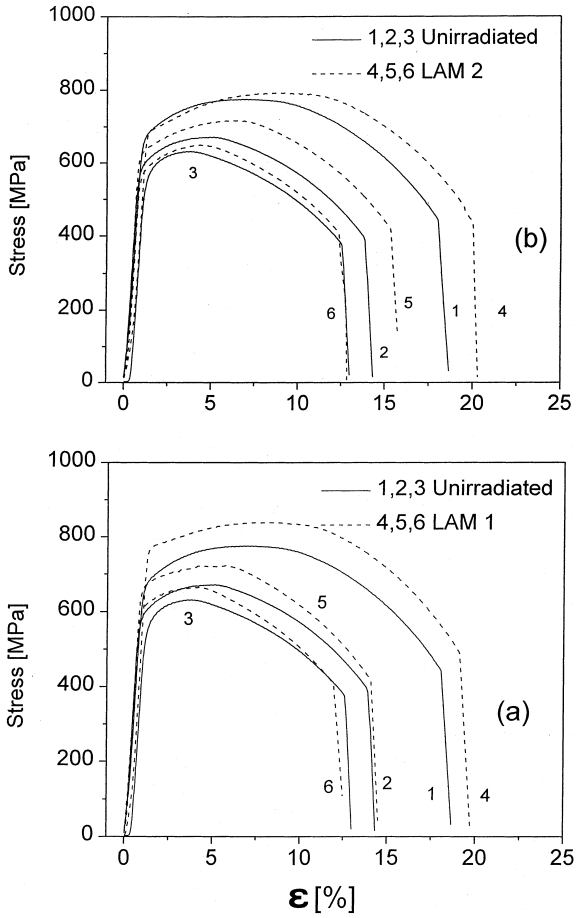

Fig. 2. The tensile curves of MANET 2 for the LAM 1 irradiation (a) and the LAM 2 irradiation (b). Test temperatures: 1&4, RT, 2&5, 250°C, 3&6, 400°C.

3.2. Impact properties

3.2.1. Results in pure iron, CETA and MANET

Fig. 3 shows the results of the Charpy impact tests for irradiated and unirradiated iron. The unirradiated material has a very sharp transition from brittle to ductile situated at −33°C. The shift of DBTT produced by the irradiations LAM 1 and LAM 2 are respectively

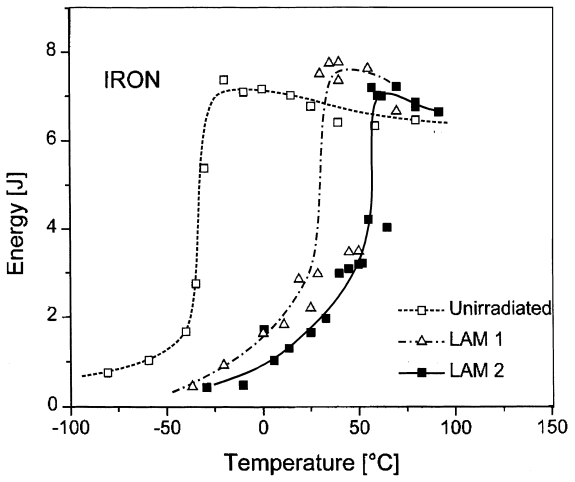

Fig. 3. Temperature dependence of the Charpy absorbed energy for iron.

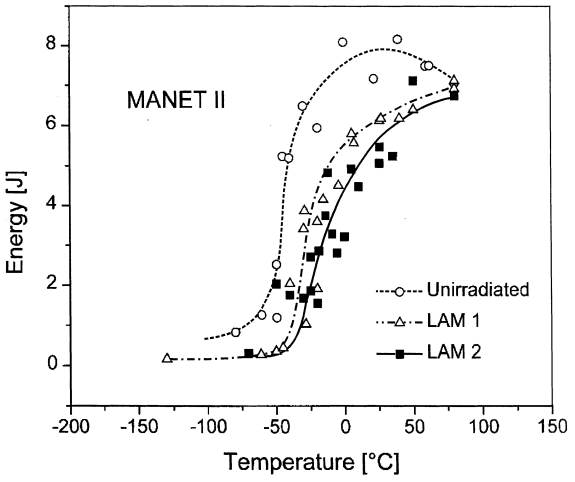

Fig. 5. Temperature dependence of the Charpy absorbed energy for MANET 2.

63°C and 90°C, reminding that LAM 2 has a three times higher dose than LAM 1. The transition brittle to ductile is taking a much wider temperature range in the irradiated material, indicating a mixed fracture with brittle and ductile zones. The SEM fractographs of the LAM 1 and LAM 2 iron specimen did not show significative differences. In the transition region (absorbed energy = 2 y), the fracture was of the transgranular cleavage type with ductile features.

The brittle–ductile transition temperature of the as quenched CETA lies at 17°C (Fig. 4). The upper shelf energy (2 J) is much reduced as compared to that of pure iron (7 J). This is due to the large amount of carbon in solution and probably also to the very high dislocation density. The shift in DBTT is 86°C for LAM 1 and 145°C for LAM 2.

The DBTT of the unirradiated MANET 2 is around −45°C as can be seen in Fig. 5. The shift of the DBTT produced by the irradiation LAM 1 is 23°C and 40°C in the case of LAM 2.

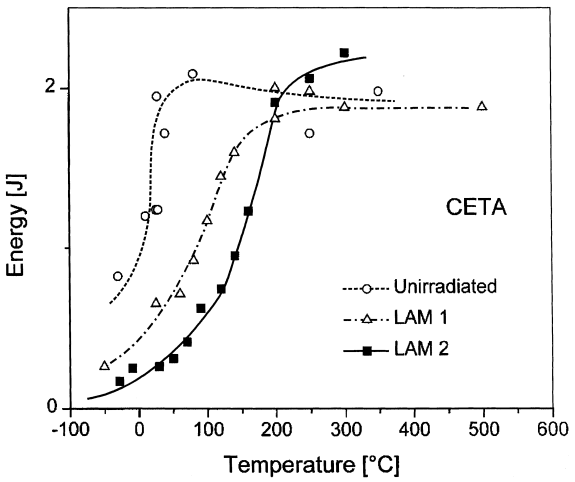

Fig. 4. Temperature dependence of the Charpy absorbed energy for CETA.

3.2.2. Structural effects and their relation with the tests results

The ductile to brittle transition (DBT) is best modelled by taking into account the dynamics of the dislocations near the crack tip and their ability to shield it [7]. In the ductile case, the dislocations emitted from sources at or near the crack tip relax the stress so quickly that interatomic bonds cannot break. In the brittle case, the time limited response of the dislocation flow will eventually give rise to stress gradients at the crack tip that can break the atomic bonds and thus start the propagation of a cleavage crack. The temperature at which it occurs depends not only on the dislocation flow dynamics but also on the crack nucleation processes involved and on the resistance to cleavage. The tensile and impact properties presented above in three distinct structures, namely ferrite, virgin martensite and tempered martensite, will be discussed accordingly to this approach. Table 3 shows the main effects on DBTT, the upper shelf energy E, its change due to irradiation ΔE_{irr} and the irradiation hardening at room temperature $\Delta\sigma_{0.2}$, all parameters given in the case of LAM 2.

Only in the case of MANET, a little reduction of the upper shelf energy is noticed after irradiation. Pure iron, which has a higher ductility at room temperature, is worst in terms of DBTT and DBTT shift, as compared with MANET. Relatively wide in the steels, the unirradiated DBT of iron (0.004 wt% N) is taking place over a

Table 3
Impact properties after the LAM 2 irradiation

	DBTT (°C)	DBTT-Shift (°C)	E_{unirr} (J)	ΔE_{irr} (J)	$\Delta\sigma_{0.2}$ (MPa)
Iron (as received)	−33	90	7.1	0	20.6
CETA (as quenched)	17	145	2	0.1	48.5
MANET (tempered)	−45	40	8	−1	15.1

range of 40°C only (see Figs. 3–5). The same sharp transition is produced in a N free low activation martensitic steel [8]. Therefore it is assumed that unsharp transitions are the result of the influence of nitrogen in this family of steels.

The advantage of using in MANET a structure with 100% (tempered) martensite in terms of a low DBTT and DBTT shift, as was shown by Kayano et al. [9], is verified in our work. The finer structure of the tempered martensite as compared with ferrite, allows for a greater amount of dislocation sources to be activated and fed to the crack tip. It has also accordingly small mean free paths for dislocation glide with short response time for stress retrieval at the crack tip. As compared with pure iron, the ferritic martensitic steel has more grain and lath boundaries which act as sinks for the point defects and thus the lesser formation of defect clusters. The virgin martensite of the CETA shows more irradiation hardening (LAM 1,RT, $\Delta\sigma_{0.2} = 243$ Mpa for CETA and 93 Mpa for MANET), probably because the sinks are saturated with light solutes (N,C). The martensitic transformation has induced a very high density of immobile dislocations inside the martensite lath and the stress level is so high that little energy is needed for rupture. The irradiation has a drastic effect in increasing even more the stress level and thus produces a large DBTT shift. Another difference in structure between the as quenched CETA and MANET 2 is the quasi-absence of carbides. The carbides which are involved in the nucleation of the cracks [10], do not affect dramatically the impact properties since MANET has the lowest DBTT, DBTT shift and the highest upper shelf energy. The comparison of the MANET 2 and the as quenched CETA is valid because these materials have very similar impact properties in the normalized and tempered condition.The DBTT measured with $55 \times 10 \times 10$ mm^3 specimen in MANET 2 and CETA is 0°C and −10°C respectively, and has a very similar shape [3].

The shift in DBTT seems to correlate with the increase of the yield stress as shown in Table 3 for the different microstructures. Nevertheless the strongest irradiation effects in terms of hardening were obtained with the LAM 1 irradiation. The LAM 2 irradiation produced the largest shift in DBTT for all materials, probably because the higher dose overtakes the effect of the low T_{irr} of LAM 1. This can be interpreted in terms of a reduction of the cleavage fracture stress, caused by the irradiation.

4. Conclusions

Three materials with very typical structures, pure iron (ferrite), two ferritic martensitic steels CETA (as quenched martensite) and MANET (tempered martensite) have been irradiated with neutrons at 250°C to 0.04 dpa and at 400°C to 0.13 dpa. The tempered martensite has demonstrated the smallest ductile–brittle transition temperature and the smallest shift after irradiation. It had also the smallest irradiation yield stress hardening. The tempered martensite derives these advantages due to its very fine structure.

Acknowledgements

Thanks are due to Drs. K. Ehrlich and M. Schirra of KFK for the supply of the steels to R. Bruetsch for the SEM analysis, to Drs. M. Lambrigger and M. Victoria for valuable comments and to Dr. W. Waeber for his help at the experiment set up. We wish to thank Dr. F. Hegedues for the reactor dosimetry and the team of Saphir and the Hot Laboratories, specially Dr. E. Lehmann, R. Christen, K. Jegerlehner and A. Christen for their help during the experiment.

References

[1] R.L. Klueh, K. Ehrlich, F. Abe, J. Nucl. Mater. 191–194 (1992) 116.
[2] D. Gavillet, P. Marmy, M. Victoria, J. Nucl. Mater. 191–194 (1992) 890.
[3] K. Ehrlich, S. Kelzenberg, H.D. Röhrig, L. Schäfer, M. Schirra, J. Nucl. Mater. 212–215 (1994) 678.
[4] R.E. Reed-Hill, Physical Metallurgy Principles, 1973, p. 728.
[5] E. Lehmann, PSI Report TM-41-94-10.
[6] D.J. Dingley, D. McLean, Acta Metall. 15 (1967) 885.
[7] S.G. Roberts, M. Ellis, P.B. Hirsch, Mater. Sci. and Eng. A 164 (1993) 135.
[8] M. Victoria, D. Gavillet, P. Spätig, F. Rezai-Aria, S. Rossmann, J. Nucl. Mater. 233–237 (1996) 326.
[9] H. Kayano, M. Narui, S. Ohta, S. Morozumi, J. Nucl. Mater. 133–134 (1985) 649.
[10] G.T. Hahn, Metall. Trans. A 15A (1984) 947.